Supplementary Information for *FaIRv2.0.0: a generalised impulse-response model for climate uncertainty and future scenario exploration*

Nicholas J. Leach[1], Stuart Jenkins[1], Zebedee Nicholls[2,3], Christopher J. Smith[4,5], John Lynch[1], Michelle Cain[1], Tristram Walsh[1], Bill Wu[1], Junichi Tsutsui[6], and Myles R. Allen[1,7]

[1]Department of Physics, Atmospheric, Oceanic, and Planetary Physics, University of Oxford, United Kingdom.
[2]Australian–German Climate and Energy College, University of Melbourne, Australia.
[3]School of Earth Sciences, University of Melbourne, Australia.
[4]School of Earth and Environment, University of Leeds, Leeds, UK.
[5]International Institute for Applied Systems Analysis, Laxenburg, Austria.
[6]Environmental Science Laboratory, Central Research Institute of Electric Power Industry, Abiko-shi, Japan.
[7]Environmental Change Institute, University of Oxford, Oxford, UK.

Correspondence: Nicholas J. Leach (nicholas.leach@stx.ox.ac.uk)

Table S1. Units used in GIR when the default parameter set is used for each gas or aerosol species. Default forcing unit for all species is Wm^{-2}.

Variable	CO_2	CH_4	N_2O	SOx	NOx	BC	OC	NH3	VOC	All other WMGHGs
Emissions	PgC	$TgCH_4$	TgN	$TgSO_2$	TgN	TgC	TgC	Tg	Tg	Tg
Concentrations	ppm	ppb	ppb	-	-	-	-	-	-	ppb

1 FaIRv2.0 parameter defaults

Table S2. FaIRv2.0 default parameter values

	a_1	a_2	a_3	a_4	τ_1	τ_2	τ_3	τ_4	r_0	r_u	r_T	r_a	PI_conc	emis2conc	f_1	f_2	f_3
bc	1.0	0	0	0	1.0	1.0	1.0	1.0	1.0	0	0	0	-	1.0	0	0.03222	0
bc|aci	-	-	-	-	-	-	-	-	-	-	-	-	-	-	0	-0.0104	0
bc|bc_on_snow	-	-	-	-	-	-	-	-	-	-	-	-	-	-	0	0.0113	0
c2f6	1.0	0	0	0	100.0	1.0	1.0	1.0	184.9	0	0	0	-	0.04077	0	0.25	0
c3f8	1.0	0	0	0	26.0	1.0	1.0	1.0	132.8	0	0	0	-	0.02993	0	0.28	0
c4f10	1.0	0	0	0	26.0	1.0	1.0	1.0	132.8	0	0	0	-	0.02364	0	0.36	0
c5f12	1.0	0	0	0	41.0	1.0	1.0	1.0	169.6	0	0	0	-	0.01953	0	0.41	0
c6f14	1.0	0	0	0	31.0	1.0	1.0	1.0	148.6	0	0	0	-	0.01664	0	0.44	0
c7f16	1.0	0	0	0	30.0	1.0	1.0	1.0	145.7	0	0	0	-	0.0145	0	0.5	0
c8f18	1.0	0	0	0	30.0	1.0	1.0	1.0	145.7	0	0	0	-	0.01284	0	0.55	0
c_c4f8	1.0	0	0	0	32.0	1.0	1.0	1.0	151.3	0	0	0	-	0.02813	0	0.32	0
carbon_dioxide	0.2173	0.224	0.2824	0.2763	inf	394.4	36.54	4.304	30.4	0.0177	2.64	0	278.0	0.4689	4.57	0	0.086
carbon_tetrachloride	1.0	0	0	0	0.32	1.0	1.0	1.0	1.794	0	0	0	2.5e-05	0.03658	0	0.174	0
carbon_tetrachloride|strat_o3	-	-	-	-	-	-	-	-	-	-	-	-	-	-	0	-0.07699	0
cf4	1.0	0	0	0	500.0	1.0	1.0	1.0	131.0	0	0	0	0.03405	0.06394	0	0.09	0
cfc11	1.0	0	0	0	0.52	1.0	1.0	1.0	2.915	0	0	0	-	0.04096	0	0.26	0
cfc113	1.0	0	0	0	0.93	1.0	1.0	1.0	5.213	0	0	0	-	0.03003	0	0.3	0
cfc113|strat_o3	-	-	-	-	-	-	-	-	-	-	-	-	-	-	0	-0.02411	0
cfc114	1.0	0	0	0	1.89	1.0	1.0	1.0	10.59	0	0	0	-	0.03292	0	0.31	0
cfc114|strat_o3	-	-	-	-	-	-	-	-	-	-	-	-	-	-	0	-0.007323	0
cfc115	1.0	0	0	0	5.4	1.0	1.0	1.0	30.27	0	0	0	-	0.03643	0	0.2	0
cfc115|strat_o3	-	-	-	-	-	-	-	-	-	-	-	-	-	-	0	-0.001333	0
cfc11|strat_o3	-	-	-	-	-	-	-	-	-	-	-	-	-	-	0	-0.05324	0
cfc12	1.0	0	0	0	1.02	1.0	1.0	1.0	5.717	0	0	0	-	0.04654	0	0.32	0
cfc12|strat_o3	-	-	-	-	-	-	-	-	-	-	-	-	-	-	0	-0.0209	0
ch2cl2	1.0	0	0	0	0.004928	1.0	1.0	1.0	0.02762	0	0	0	0.006913	0.06625	0	0.028	0
ch3ccl3	1.0	0	0	0	0.05	1.0	1.0	1.0	0.2803	0	0	0	-	0.04218	0	0.07	0
ch3ccl3|strat_o3	-	-	-	-	-	-	-	-	-	-	-	-	-	-	0	-0.08305	0
chcl3	1.0	0	0	0	0.00501	1.0	1.0	1.0	0.02808	0	0	0	0.006	0.04714	0	0.07	0
co	1.0	0	0	0	1.0	1.0	1.0	1.0	1.0	0	0	0	-	1.0	0	0	0
co|trop_o3	-	-	-	-	-	-	-	-	-	-	-	-	-	-	0	0.00012	0
halon1202	1.0	0	0	0	0.025	1.0	1.0	1.0	0.1401	0	0	0	-	0.02682	0	0.27	0
halon1202|strat_o3	-	-	-	-	-	-	-	-	-	-	-	-	-	-	0	-1.882	0
halon1211	1.0	0	0	0	0.16	1.0	1.0	1.0	0.8968	0	0	0	4.447e-06	0.03403	0	0.29	0
halon1211|strat_o3	-	-	-	-	-	-	-	-	-	-	-	-	-	-	0	-1.263	0
halon1301	1.0	0	0	0	0.72	1.0	1.0	1.0	4.036	0	0	0	-	0.03779	0	0.3	0
halon1301|strat_o3	-	-	-	-	-	-	-	-	-	-	-	-	-	-	0	-0.6575	0
halon2402	1.0	0	0	0	0.28	1.0	1.0	1.0	1.569	0	0	0	-	0.02166	0	0.31	0
halon2402|strat_o3	-	-	-	-	-	-	-	-	-	-	-	-	-	-	0	-1.552	0
hcfc141b	1.0	0	0	0	0.094	1.0	1.0	1.0	0.5269	0	0	0	-	0.04812	0	0.16	0
hcfc141b|strat_o3	-	-	-	-	-	-	-	-	-	-	-	-	-	-	0	-0.02533	0
hcfc142b	1.0	0	0	0	0.18	1.0	1.0	1.0	1.009	0	0	0	-	0.05599	0	0.19	0
hcfc142b|strat_o3	-	-	-	-	-	-	-	-	-	-	-	-	-	-	0	-0.006152	0
hcfc22	1.0	0	0	0	0.119	1.0	1.0	1.0	0.667	0	0	0	-	0.06507	0	0.21	0
hcfc22|strat_o3	-	-	-	-	-	-	-	-	-	-	-	-	-	-	0	-0.006746	0
hfc125	1.0	0	0	0	0.3	1.0	1.0	1.0	1.682	0	0	0	-	0.04688	0	0.23	0
hfc134a	1.0	0	0	0	0.14	1.0	1.0	1.0	0.7847	0	0	0	-	0.05515	0	0.16	0
hfc143a	1.0	0	0	0	0.51	1.0	1.0	1.0	2.859	0	0	0	-	0.06695	0	0.16	0
hfc152a	1.0	0	0	0	0.016	1.0	1.0	1.0	0.08968	0	0	0	-	0.08519	0	0.1	0
hfc227ea	1.0	0	0	0	0.36	1.0	1.0	1.0	2.018	0	0	0	-	0.03309	0	0.26	0
hfc23	1.0	0	0	0	2.28	1.0	1.0	1.0	12.78	0	0	0	-	0.08037	0	0.18	0
hfc236fa	1.0	0	0	0	2.13	1.0	1.0	1.0	11.94	0	0	0	-	0.03701	0	0.24	0
hfc245fa	1.0	0	0	0	0.079	1.0	1.0	1.0	0.4428	0	0	0	-	0.04197	0	0.24	0
hfc32	1.0	0	0	0	0.054	1.0	1.0	1.0	0.3027	0	0	0	-	0.1082	0	0.11	0
hfc365mfc	1.0	0	0	0	0.089	1.0	1.0	1.0	0.4989	0	0	0	-	0.038	0	0.22	0
hfc4310mee	1.0	0	0	0	0.17	1.0	1.0	1.0	0.9529	0	0	0	-	0.02232	0	0.359	0
methane	1.0	0	0	0	8.8	1.0	1.0	1.0	8.8	0	-0.33	0.00032	720.0	0.3517	0	0	0.0385
methane|strat_h2o	-	-	-	-	-	-	-	-	-	-	-	-	-	-	0	5.5e-05	0
methane|trop_o3	-	-	-	-	-	-	-	-	-	-	-	-	-	-	0	0.000133	0
methyl_bromide	1.0	0	0	0	0.008	1.0	1.0	1.0	0.04484	0	0	0	0.0053	0.05927	0	0.004	0
methyl_bromide|strat_o3	-	-	-	-	-	-	-	-	-	-	-	-	-	-	0	-1.972	0
methyl_chloride	1.0	0	0	0	0.009	1.0	1.0	1.0	0.05045	0	0	0	0.457	0.1114	0	0.004	0
methyl_chloride|strat_o3	-	-	-	-	-	-	-	-	-	-	-	-	-	-	0	-0.04614	0
nf3	1.0	0	0	0	5.69	1.0	1.0	1.0	31.89	0	0	0	-	0.07925	0	0.2	0
nh3	1.0	0	0	0	1.0	1.0	1.0	1.0	1.0	0	0	0	-	1.0	0	0	0
nitrous_oxide	1.0	0	0	0	109.0	1.0	1.0	1.0	65.45	0	0	0	270.0	0.201	0	0	0.107
nmvoc	1.0	0	0	0	1.0	1.0	1.0	1.0	1.0	0	0	0	-	1.0	0	0	0
nmvoc|trop_o3	-	-	-	-	-	-	-	-	-	-	-	-	-	-	0	0.00026	0
nox	1.0	0	0	0	1.0	1.0	1.0	1.0	1.0	0	0	0	-	1.0	0	0	0
nox_avi	1.0	0	0	0	1.0	1.0	1.0	1.0	1.0	0	0	0	-	1.0	0	0	0
nox_avi|contrails	-	-	-	-	-	-	-	-	-	-	-	-	-	-	0	0.0115	0
nox|trop_o3	-	-	-	-	-	-	-	-	-	-	-	-	-	-	0	0.00098	0
oc	1.0	0	0	0	1.0	1.0	1.0	1.0	1.0	0	0	0	-	1.0	0	-0.009421	0
oc|aci	-	-	-	-	-	-	-	-	-	-	-	-	-	-	0	-0.0104	0
sf6	1.0	0	0	0	32.0	1.0	1.0	1.0	151.3	0	0	0	-	0.03852	0	0.57	0
so2	1.0	0	0	0	1.0	1.0	1.0	1.0	1.0	0	0	0	204.0	1.0	0	-0.002444	0
so2f2	1.0	0	0	0	0.36	1.0	1.0	1.0	2.018	0	0	0	-	0.05513	0	0.2	0
so2|aci	-	-	-	-	-	-	-	-	-	-	-	-	-	-	-1.69	0	0

Table S3. GWP metric for default parameter values computed against a baseline emission scenario that reproduces historical concentrations (Meinshausen et al., 2017) up to 2014, then the fixed 2014 value following. These are calculated using the change in ERF arising from a 1 t emission pulse in 2015. To compute the “direct” GWP value, we use the change in the direct ERF of each agent (ie. corresponding to the parameters without a “|” in their name in table S2). To compute the “indirect” GWP value, we use the change in the total ERF arising from the emission pulse of the agent. Hence the “indirect” GWP value will include effects such as changes to CO_2 uptake due to differences in the temperature responses of the baseline and perturbed runs. For ozone depleting substances, the “indirect” value includes ERF changes arising from ozone depletion. For aerosols, the “direct” value includes the radiation interaction component only, while the “indirect” value also includes cloud interaction. We emphasize that these values do not represent new estimates for the value of the GWP metric and are intended for reference and model comparison.

Time horizon / yrs	5		10		20		50		100		500	
metric type	direct	indirect	direct	indirect	direct	indirect	direct	indirect	direct	indirect	direct	indirect
Gas name												
bc	4510	4650	2610	2710	1490	1550	696	746	381	425	86.8	121
c2f6	7890	7900	8680	8700	9640	9610	11100	11100	12100	12100	13400	13600
c3f8	6480	6490	7120	7140	7900	7870	9050	9030	9780	9790	10300	10400
c4f10	6580	6590	7240	7250	8020	7990	9190	9170	9930	9950	10400	10500
c5f12	6200	6210	6810	6830	7560	7530	8680	8660	9410	9420	10200	10300
c6f14	5660	5670	6230	6240	6910	6870	7930	7890	8570	8560	9120	9210
c7f16	5610	5620	6170	6180	6840	6800	7840	7810	8480	8470	9000	9110
c8f18	5460	5470	6010	6030	6660	6700	7640	7740	8260	8410	8770	9060
c_c4f8	6960	6970	7660	7670	8490	8460	9740	9730	10500	10600	11200	11400
carbon_dioxide	1.0	0.999	1.0	0.997	1.0	0.994	1.0	0.989	1.0	0.987	1.0	0.981
carbon_tetrachloride	4520	2530	4620	2580	4450	2500	3490	1980	2310	1340	549	374
cf4	4450	4460	4900	4920	5440	5480	6270	6350	6840	6950	7720	7950
cfc11	7820	6230	8210	6550	8330	6590	7430	5870	5610	4420	1490	1130
cfc113	6770	6240	7260	6690	7650	7000	7580	6940	6550	6000	2250	2030
cfc114	7790	7610	8460	8280	9150	8910	9770	9530	9420	9230	4830	4820
cfc115	5610	5580	6150	6120	6760	6680	7590	7500	7910	7840	6400	6430
cfc12	11200	10500	12100	11200	12800	11800	12800	11800	11300	10400	4060	3720
ch2cl2	129	129	74.2	74.7	42.2	42.9	19.8	20.6	10.8	11.7	2.46	3.34
ch3ccl3	1380	-258.0	1050	-197.0	670	-126.0	319	-61.5	175	-34.9	39.8	-9.75
chcl3	233	233	134	135	76.3	77.6	35.7	37.3	19.6	21.2	4.45	6.04
co	0	16.9	0	9.8	0	5.63	0	2.7	0	1.54	0	0.437
halon1202	2260	-13500.0	1450	-8690.0	835	-5060.0	391	-2430.0	214	-1380.0	48.8	-382.0
halon1211	6460	-21700.0	6160	-20700.0	5260	-17800.0	3270	-11200.0	1870	-6600.0	425	-1800.0
halon1301	8450	-10100.0	8990	-10700.0	9330	-11200.0	8890	-10700.0	7270	-8920.0	2200	-3050.0
halon2402	4720	-18900.0	4770	-19200.0	4500	-18200.0	3390	-13800.0	2160	-9040.0	506	-2490.0
hcfc141b	4500	3800	3950	3340	2960	2520	1560	1350	857	767	195	212
hcfc142b	7090	6870	6860	6660	6010	5860	3890	3840	2260	2300	516	627
hcfc22	8460	8200	7730	7500	6160	5940	3460	3300	1920	1810	438	348
hfc125	7620	7630	7750	7770	7390	7370	5690	5660	3690	3690	872	875
hfc134a	5640	5650	5290	5300	4380	4420	2600	2660	1460	1540	333	423
hfc143a	7860	7870	8250	8270	8350	8320	7420	7400	5570	5560	1470	1470
hfc152a	1850	1860	1100	1110	629	639	294	307	161	174	36.7	49.4
hfc227ea	6170	6180	6360	6380	6210	6250	5050	5130	3440	3580	835	1010
hfc23	11100	11100	12000	12000	13100	13000	14200	14000	13900	13900	7900	8000
hfc236fa	6790	6800	7380	7400	8010	7980	8630	8610	8420	8430	4610	4680
hfc245fa	5610	5620	4740	4760	3400	3430	1720	1770	942	1000	214	278
hfc32	5760	5770	4460	4480	2900	2930	1390	1430	760	815	173	227
hfc365mfc	4820	4830	4180	4190	3090	3120	1600	1650	881	937	200	259
hfc4310mee	5290	5300	5090	5110	4400	4440	2790	2860	1610	1690	367	463
methane	95.0	135	85.3	122	66.1	95.3	35.8	52.9	19.7	30.2	4.44	8.33
methyl_bromide	26.7	-13200.0	15.4	-7630.0	8.75	-4380.0	4.1	-2100.0	2.24	-1200.0	0.511	-333.0
methyl_chloride	56.3	-595.0	32.6	-345.0	18.5	-198.0	8.67	-95.2	4.75	-54.2	1.08	-15.4
nf3	12200	12200	13400	13300	14700	14600	16500	16400	17300	17300	14200	14400
nh3	0	0	0	0	0	0	0	0	0	0	0	0
nitrous_oxide	286	286	307	308	326	328	330	335	294	302	110	125
nmvoc	0	36.5	0	21.2	0	12.2	0	5.86	0	3.33	0	0.947
nox	0	138	0	80.1	0	46.0	0	22.1	0	12.6	0	3.57
nox_avi	0	1620	0	940	0	539	0	259	0	147	0	41.9
oc	-1320.0	-2790.0	-764.0	-1620.0	-435.0	-930.0	-204.0	-446.0	-112.0	-254.0	-25.4	-72.1
sf6	17000	17000	18700	18600	20700	20600	23800	23700	25700	25800	27400	27800
so2	-342.0	-1090.0	-198.0	-634.0	-113.0	-364.0	-52.8	-175.0	-28.9	-99.4	-6.58	-28.2
so2f2	7910	7920	8150	8170	7950	7930	6470	6440	4410	4390	1070	1020

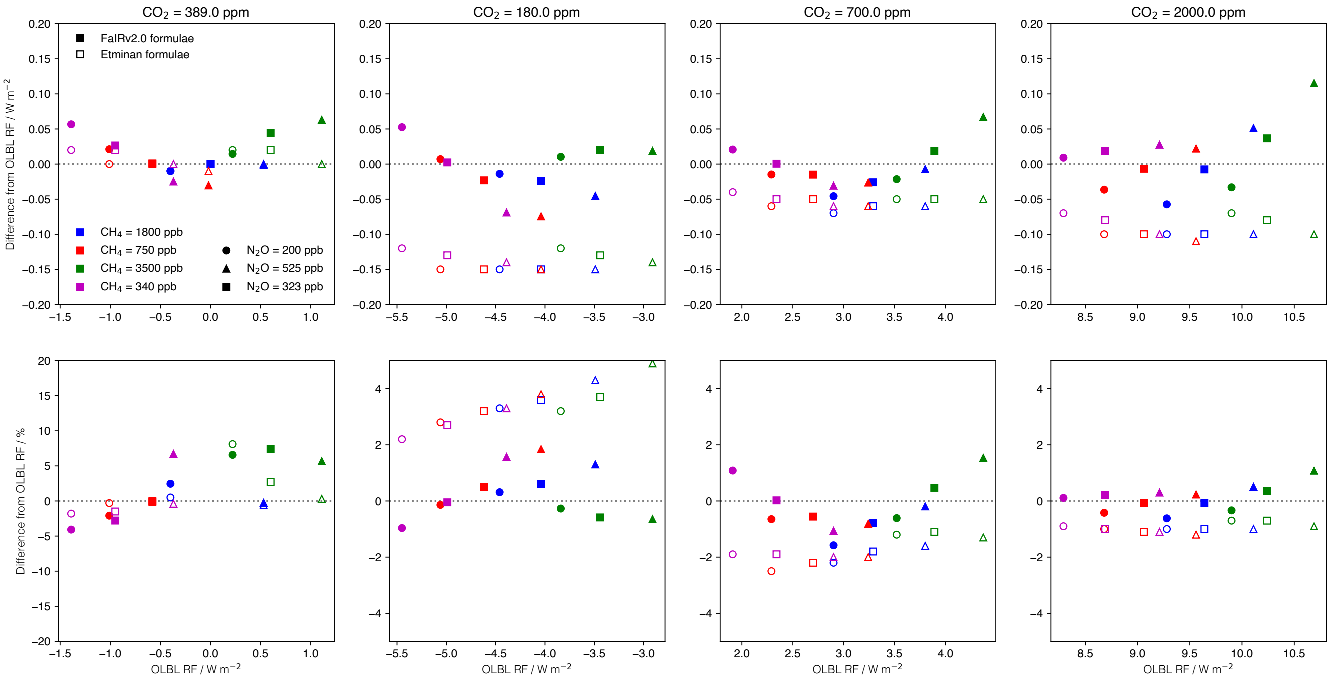

Figure S1. Comparison of the CO_2, CH_4 and N_2O ERF relationships used in FaIRv2.0 to the simple formulae and OLBL data from (Etminan et al., 2016). Top row shows absolute differences, grouped by CO_2 concentrations. Bottom row shows differences as a percentage of total forcing, again grouped by CO_2 concentration.

2 Radiative forcing of carbon dioxide, methane and nitrous oxide

Here we compare the concentration-forcing relationships of CO_2, CH_4 and N_2O used in FaIRv2.0, which exclude the interaction terms between gases, to the standard simple formulae detailed in Etminan et al. (2016). Figure SS1 shows a comparison of the Oslo line-by-line (OLBL) data from Etminan et al. to both the Etminan et al. formulae and those used in FaIRv2.0. The main difference between the relationships used in FaIRv2.0 and those in Etminan et al. is the variance in the error when compared to the OLBL. The FaIRv2.0 relationships have a larger error variance at each CO_2 concentration than the Etminan et al. formulae (fig SS1). This is due to the lack of interaction terms, and results in a maximum absolute error of 0.115 W m^{-2} at concentrations of $CO_2 = 2000$ ppm, $CH_4 = 3500$ ppm, and $N_2O = 525$ ppm (the green triangle in the far right-hand side subplot in figure SS1). We believe that in the context of other uncertainties associated with such a high concentration scenario this error is defensible. We note (as was done in Etminan et al.) that the absolute uncertainty in the OLBL calculation is estimated to be 10% for CO_2 and N_2O and 14% for CH_4.

3 CMIP6 data pre-processing

Here we detail the steps taken to remove model drift from and pre-process the CMIP6 data used throughout the study.

3.1 Drift correction and baseline estimation

For each model ensemble member, we find the associated parent experiment (a piControl run, not necessarily of the same ensemble member) and branch time in the Dataset Metadata. For each of the abrupt-4xCO2 and 1pctCO2 experiments, the model drift is estimated as the slope of a linear regression of the parent experiment against time, starting at the branch year, for a period equal to the duration of the experiment; and the baseline temperature of the experiment is estimated as the value of the regression at the branch point. If the parent experiment ends "before" the experiment ends, then the end of the linear regression is set as the end of the parent experiment and the start moves before the branch point accordingly such that the regression period is still equal to the duration of the experiment. For example, if the experiment is 150 years long, and was branched in year 200 out of a 300-year piControl, the drift would be estimated as the slope of a linear regression over years 150-300 of the piControl; and the experiment baseline temperature is the value of the regression line at year 200. This drift correction procedure is applied to both the surface temperature and top-of-atmosphere radiative flux variables for the abrupt-4xCO2 experiment. For the 1pctCO2 experiment, we remove the estimated model drift as described above, but estimate the baseline temperature as the intercept of a linear regresion over the first 25 years of the experiment following Sanderson (2020). For the SSP experiment data shown (eg. in figure 9), we do not apply any drift correction.

3.2 Other pre-processing

After applying the drift correction to each ensemble member (if applicable), we then average over all available ensemble members of each model to obtain the data used in fitting parameters, or shown in the figures. The number of ensemble members per model is shown in the table below.

Table S4. Number of ensemble members used per CMIP6 model.

model	abrupt-4xCO2	1pctCO2	ssp119	ssp126	ssp245	ssp370	ssp585
ACCESS-CM2	1	1	0	3	3	3	3
ACCESS-ESM1-5	1	1	0	3	3	3	3
AWI-CM-1-1-MR	1	1	0	0	0	0	0
BCC-CSM2-MR	1	1	0	1	1	1	1
BCC-ESM1	1	1	0	0	0	3	0
CAMS-CSM1-0	2	2	2	2	2	2	2
CESM2	1	1	0	3	3	3	3
CESM2-FV2	1	1	0	0	0	0	0
CESM2-WACCM	1	1	0	1	3	3	3
CESM2-WACCM-FV2	1	1	0	0	0	0	0
CIESM	1	1	0	1	1	0	1
CNRM-CM6-1	1	1	0	6	10	6	6
CNRM-CM6-1-HR	1	1	0	1	1	1	1
CNRM-ESM2-1	3	10	5	5	5	5	5
CanESM5	2	6	50	50	50	50	50
E3SM-1-0	1	1	0	0	0	0	0
EC-Earth3-Veg	1	1	3	5	6	4	5
GFDL-CM4	1	1	0	0	1	0	1
GFDL-ESM4	1	1	1	1	3	1	1
GISS-E2-1-G	4	5	2	1	10	10	1
GISS-E2-1-H	1	1	0	0	0	0	0
GISS-E2-2-G	1	1	0	0	0	0	0
HadGEM3-GC31-LL	1	4	0	1	4	0	4
HadGEM3-GC31-MM	1	1	0	1	0	0	3
INM-CM4-8	1	1	0	1	1	1	1
INM-CM5-0	1	1	0	1	1	5	1
IPSL-CM6A-LR	1	1	6	6	11	11	6
KACE-1-0-G	1	1	0	3	3	3	3
MIROC-ES2L	1	1	3	3	1	1	1
MIROC6	1	1	1	3	50	3	50
MPI-ESM1-2-HR	1	1	0	2	2	10	2
MPI-ESM1-2-LR	1	1	0	10	10	10	10
MRI-ESM2-0	4	2	1	1	5	5	1
NESM3	1	1	0	2	2	0	2
NorCPM1	1	1	0	0	0	0	0
NorESM2-LM	1	1	0	1	3	3	1
NorESM2-MM	1	1	0	1	1	1	1
SAM0-UNICON	1	1	0	0	0	0	0
TaiESM1	1	1	0	0	0	0	0
UKESM1-0-LL	1	4	5	13	5	13	5
CAS-ESM2-0	0	1	0	0	0	0	0
CMCC-CM2-SR5	0	1	0	1	1	1	1
CanESM5-CanOE	0	1	0	3	3	3	3
FGOALS-f3-L	0	3	0	1	1	1	1
FGOALS-g3	0	3	0	1	1	1	4
FIO-ESM-2-0	0	3	0	3	3	0	3
IITM-ESM	0	1	0	0	0	0	0
MCM-UA-1-0	0	1	0	1	1	1	1
MPI-ESM-1-2-HAM	0	1	0	0	0	2	0
EC-Earth3	0	0	1	7	16	5	7
Total models / experiment	40	49	12	36	36	33	37

4 Energy balance model parameters

Using the method described in Cummins et al. (2020), we tune parameters to CMIP6 models for a 3-box version of the energy balance model described in Geoffroy et al. (2013), with the ocean heat uptake efficacy factor as Winton et al. (2010) included.

Table S5. CMIP6 tuned 3-box energy balance model parameters

	γ	C_1	C_2	C_3	λ	κ_2	κ_3	ϵ
ACCESS-CM2	1.6190	3.761	11.1100	8.269000e+01	0.6728	3.0130	0.6887	1.349000
ACCESS-ESM1-5	2.7730	3.805	8.7790	8.518000e+01	0.6992	3.6990	0.8399	1.565000
AWI-CM-1-1-MR	4.0820	4.225	10.6000	4.705000e+01	1.1690	1.9030	0.6938	1.414000
BCC-CSM2-MR	2.4290	5.157	12.2800	6.665000e+01	0.9237	2.3970	0.9602	1.405000
BCC-ESM1	1.9080	5.655	16.4600	7.727000e+01	0.8828	1.5120	0.9629	1.283000
CAMS-CSM1-0	26.8600	3.482	7.6360	5.606000e+01	1.8650	6.1150	0.6972	1.241000
CESM2	2.6530	5.796	54.9800	9.084000e+01	0.4100	0.9218	0.2440	1.358000
CESM2-FV2	2.7130	3.758	7.0540	8.885000e+01	0.5497	3.8790	0.9923	1.741000
CESM2-WACCM	2.9960	3.733	6.1820	8.724000e+01	0.7171	6.8640	0.8234	1.596000
CESM2-WACCM-FV2	2.9130	3.371	9.4840	1.079000e+02	0.5598	3.5130	0.9454	1.506000
CIESM	0.8127	5.245	11.2100	6.379000e+01	0.6931	2.6240	0.9652	1.348000
CNRM-CM6-1	4.4840	4.210	16.9000	4.185000e+02	1.2520	1.2360	0.4050	0.187800
CNRM-CM6-1-HR	6.3770	4.159	11.4700	8.655000e+01	1.0180	1.9860	0.6453	0.704900
CNRM-ESM2-1	3.7910	4.709	11.0100	1.064000e+02	0.6646	1.5080	0.7768	0.920700
CanESM5	3.6560	3.935	11.3500	7.268000e+01	0.6359	2.1240	0.6239	1.095000
E3SM-1-0	3.0600	3.654	9.5270	4.343000e+01	0.5771	2.3750	0.3653	1.515000
EC-Earth3-Veg	26.1800	3.413	10.0500	2.957000e+01	0.8413	2.4430	0.6428	1.287000
GFDL-CM4	2.7680	5.459	0.1613	7.902000e+01	1.0150	2.0460	1.8810	1.780000
GFDL-ESM4	4.0760	4.278	10.4000	1.249000e+02	1.5790	1.7640	0.7689	0.822900
GISS-E2-1-G	1.0610	3.935	10.5500	1.739000e+02	1.5130	2.0890	1.1660	1.068000
GISS-E2-1-H	2.4700	4.660	24.5300	3.198000e+07	1.6780	1.2500	0.2885	0.000733
GISS-E2-2-G	2.3470	3.613	10.9600	4.384000e+02	2.0730	1.9590	0.5838	0.329400
HadGEM3-GC31-LL	3.1200	3.817	9.3530	6.763000e+01	0.6122	2.7760	0.6352	1.172000
HadGEM3-GC31-MM	3.1180	3.476	14.2200	6.213000e+01	0.6601	2.0260	0.7008	1.024000
INM-CM4-8	2.4800	4.306	9.5960	2.027000e+01	1.5800	1.8760	0.5367	1.477000
INM-CM5-0	1.9150	4.438	11.0000	4.584000e+01	1.5710	1.8660	0.5575	1.413000
IPSL-CM6A-LR	3.2530	2.965	14.1400	6.979000e+01	0.6874	1.8100	0.4502	1.374000
KACE-1-0-G	1.9020	0.982	11.1700	1.180000e+02	0.7261	27.7700	0.9366	1.246000
MIROC6	2.2020	3.781	17.0300	1.779000e+02	1.4470	1.7410	1.1070	1.176000
MPI-ESM1-2-HR	2.9040	5.201	23.2600	7.145000e+01	1.1860	1.5940	1.0890	1.531000
MPI-ESM1-2-LR	2.2430	6.466	49.4100	1.575000e+06	1.7270	0.8626	0.2811	0.407300
MRI-ESM2-0	1.6290	4.907	10.8100	9.678000e+01	1.1190	2.3480	1.3580	1.279000
NESM3	2.8310	2.516	19.2000	1.146000e+02	0.9230	1.0370	0.4592	0.757500
NorCPM1	1.1690	7.160	35.9900	5.470000e+07	1.5480	1.2060	0.4017	0.507700
SAM0-UNICON	2.4450	4.578	6.3010	1.111000e+02	1.0320	2.6630	1.0110	1.274000
TaiESM1	2.0330	5.074	8.9460	8.662000e+01	0.8827	2.2900	0.9088	1.229000
UKESM1-0-LL	3.5760	2.984	11.2400	6.968000e+01	0.6533	2.6840	0.6245	1.138000
MIROC-ES2L	0.0140	10.040	21.1900	2.550000e+02	1.6510	0.9538	0.8993	0.594300
NorESM2-LM	1.0280	3.730	175.5000	1.448000e+00	0.7494	3.2310	1.3360	445.100000
NorESM2-MM	1.3830	4.129	128.3000	5.881000e-01	1.9660	1.4410	0.7010	207.500000

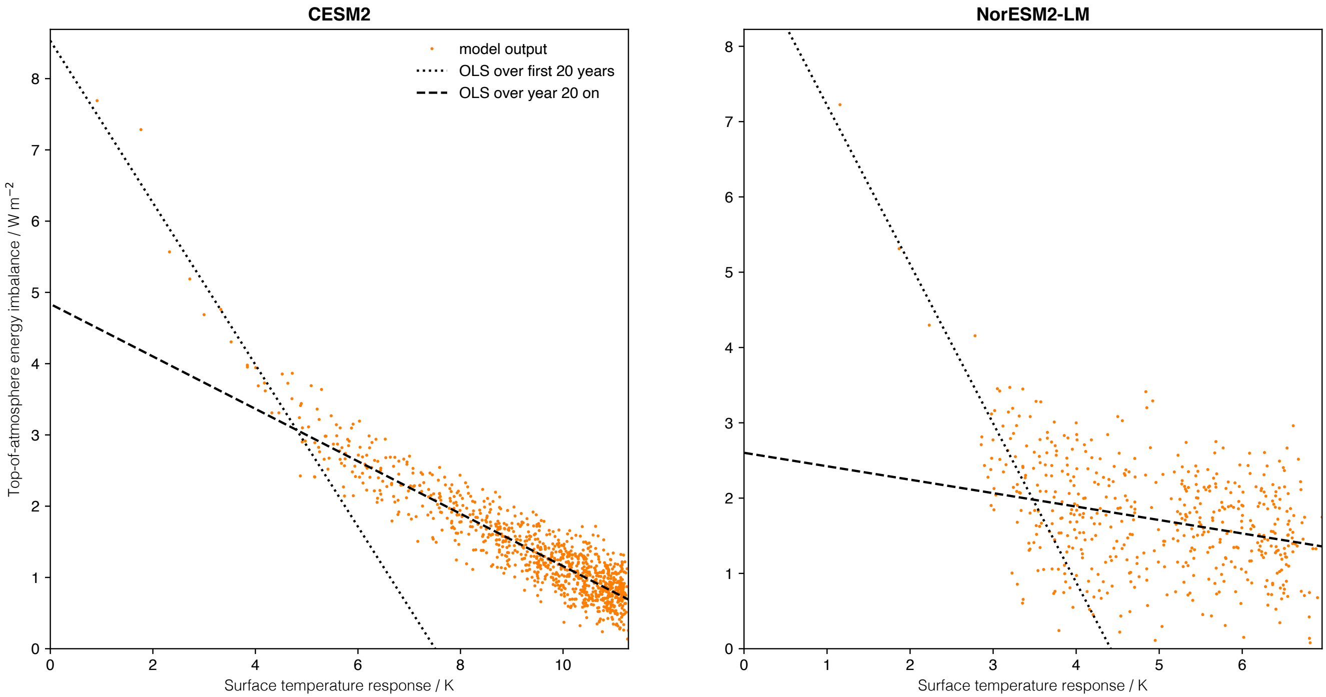

Figure S2. Gregory plots over the abrupt-4xCO2 experiment for CESM2 and NorESM2-LM. The dotted line shows the result of a linear regression over the first 20 years of the experiment, while the dashed line shows the result if instead the regression is carried out from year 20 onwards.

5 Gregory plots for CESM2 and NorESM2-LM

In fig SS2 we show Gregory plots (Gregory et al., 2002) for CESM2 and NorESm2-LM to support the discussion in section 3.1.

6 Global Warming Index calculation

The Global Warming Index follows the methodology in Haustein et al. (2016), but updates several components. We use the mean of 5 datasets for the observed warming, with associated uncertainty taken from the HadCRUT4 ensemble (Lenssen et al., 2019; Cowtan and Way, 2014; Vose et al., 2012; Morice et al., 2011; Rohde et al., 2013). We then generate 4000 realisations of historical ERF as follows. For all forcings excluding aerosol forcing, we take the best-estimate historical timeseries from Smith (2020), and scale them by factors drawn from the distributions detailed in table 6. For aerosol forcing, we take the best-estimate historical timeseries of ERFaci and ERFari, and scale them by scaling factors drawn from a skew-normal distribution that matches the quantiles of the constrained ERFaci and ERFari distributions stated in table 4 of Smith et al. (2020). We consider 18 different response model parameterisations, spanning the ranges of possible realised warming fraction (Millar et al., 2015) and response timescale (Geoffroy et al., 2013). Finally, we include uncertainty due to internal variability through timeseries from the piControl experiment of different CMIP6 models, rejecting models with a too large drift; resulting in 51 different representations of internal variability. Combining these sources of uncertainty results in a 367,200,000 member ensemble of the global warming index, from which we derive the 5-95% ranges used to constrain the FULL ensemble in the main text.

7 ALTERNATIVE ensemble variable correlations

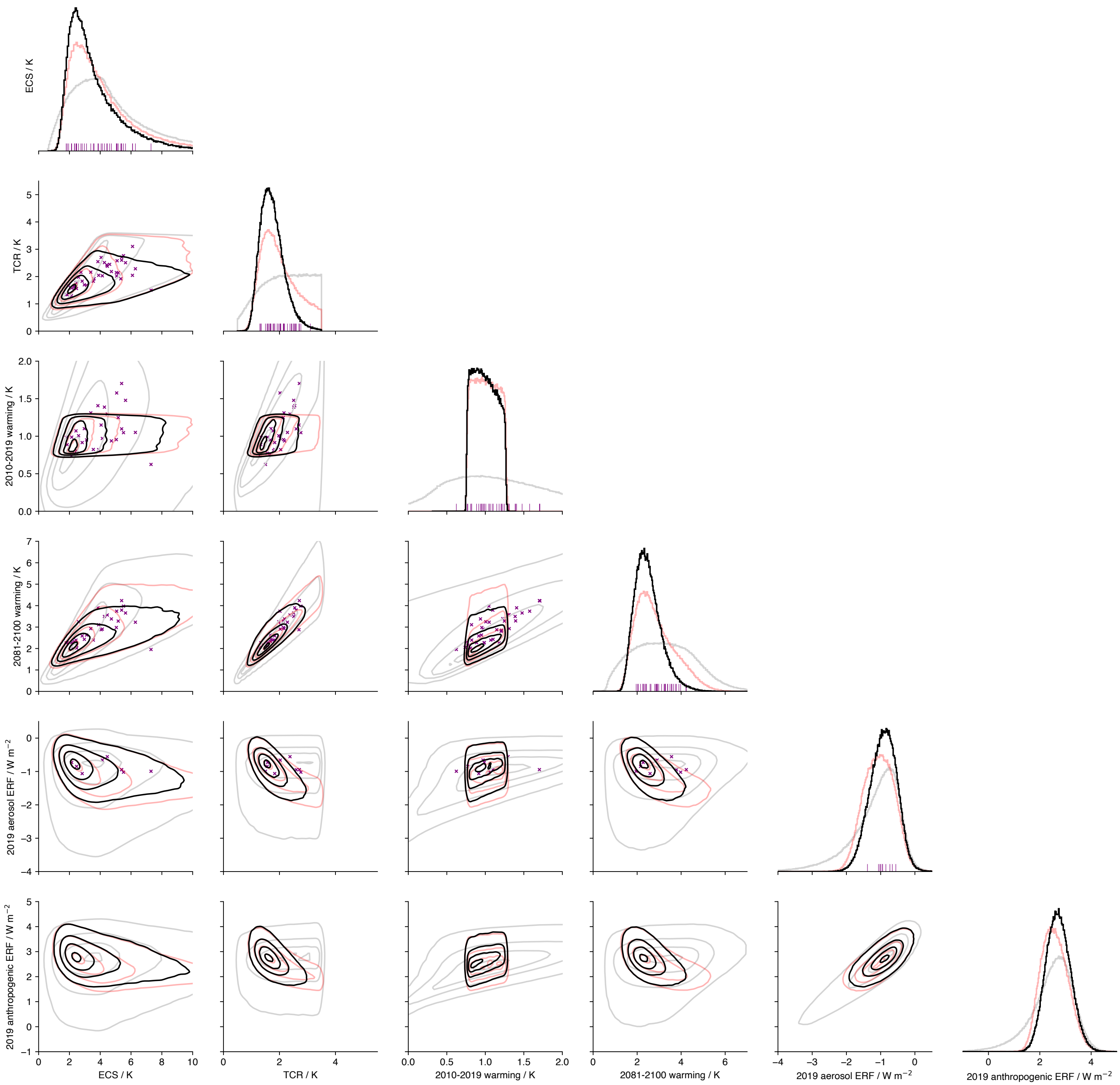

Figure S3. Corner plot depiction of the ALTERNATIVE prior and posterior ensembles as described in the main text. Diagonal plots show marginal probability density functions of each key variable; the prior shown in grey, ALTERNATIVE in black, and the prior constrained by the current level of warming only in red. Subdiagonal plots show contour plots of gaussian kernel density estimates of joint probability density. Contours show indicate regions containing 95, 67, 33 and 5 % of the ensemble members. Purple crosses and lines indicate the positions of individual CMIP6 models.

Code and data availability. The code used to produce the figures is publicly available at https://github.com/njleach/GIR. However, we stress that the code here is *not* a model release. This update to the FaIR model will be made available at https://github.com/OMS-NetZero/FAIR when fully integrated and tested. All data used in this study is publicly available at the relevant cited sources.

References

Cowtan, K. and Way, R. G.: Coverage bias in the HadCRUT4 temperature series and its impact on recent temperature trends, Quarterly Journal of the Royal Meteorological Society, 140, 1935–1944, https://doi.org/10.1002/qj.2297, http://doi.wiley.com/10.1002/qj.2297, 2014.

Cummins, D. P., Stephenson, D. B., and Stott, P. A.: Optimal Estimation of Stochastic Energy Balance Model Parameters, Journal of Climate, pp. JCLI–D–19–0589.1, https://doi.org/10.1175/JCLI-D-19-0589.1, http://journals.ametsoc.org/doi/10.1175/JCLI-D-19-0589.1, 2020.

Etminan, M., Myhre, G., Highwood, E. J., and Shine, K. P.: Radiative forcing of carbon dioxide, methane, and nitrous oxide: A significant revision of the methane radiative forcing, Geophysical Research Letters, 43, 12,614–12,623, https://doi.org/10.1002/2016GL071930, http://doi.wiley.com/10.1002/2016GL071930, 2016.

Geoffroy, O., Saint-Martin, D., Olivié, D. J. L., Voldoire, A., Bellon, G., Tytéca, S., Geoffroy, O., Saint-Martin, D., Olivié, D. J. L., Voldoire, A., Bellon, G., and Tytéca, S.: Transient Climate Response in a Two-Layer Energy-Balance Model. Part I: Analytical Solution and Parameter Calibration Using CMIP5 AOGCM Experiments, Journal of Climate, 26, 1841–1857, https://doi.org/10.1175/JCLI-D-12-00195.1, http://journals.ametsoc.org/doi/abs/10.1175/JCLI-D-12-00195.1http://journals.ametsoc.org/jcli/article-pdf/26/6/1841/4002942/jcli-d-12-00195{_}1.pdf, 2013.

Gregory, J. M., Stouffer, R. J., Raper, S. C. B., Stott, P. A., and Rayner, N. A.: An Observationally Based Estimate of the Climate Sensitivity, Journal of Climate, 15, 3117–3121, https://doi.org/10.1175/1520-0442(2002)015<3117:AOBEOT>2.0.CO;2, http://journals.ametsoc.org/doi/abs/10.1175/1520-0442{%}282002{%}29015{%}3C3117{%}3AAOBEOT{%}3E2.0.CO{%}3B2, 2002.

Haustein, K., L Otto, F. E., Uhe, P., Schaller, N., Allen, M. R., Hermanson, L., Christidis, N., McLean, P., and Cullen, H.: Real-time extreme weather event attribution with forecast seasonal SSTs, Environ. Res. Lett, 11, 64 006, https://doi.org/10.1088/1748-9326/11/6/064006, 2016.

Lenssen, N. J. L., Schmidt, G. A., Hansen, J. E., Menne, M. J., Persin, A., Ruedy, R., and Zyss, D.: Improvements in the uncertainty model in the Goddard Institute for Space Studies Surface Temperature (GISTEMP) analysis, Journal of Geophysical Research: Atmospheres, p. 2018JD029522, https://doi.org/10.1029/2018JD029522, https://onlinelibrary.wiley.com/doi/abs/10.1029/2018JD029522, 2019.

Meinshausen, M., Vogel, E., Nauels, A., Lorbacher, K., Meinshausen, N., Etheridge, D. M., Fraser, P. J., Montzka, S. A., Rayner, P. J., Trudinger, C. M., Krummel, P. B., Beyerle, U., Canadell, J. G., Daniel, J. S., Enting, I. G., Law, R. M., Lunder, C. R., O'Doherty, S., Prinn, R. G., Reimann, S., Rubino, M., Velders, G. J. M., Vollmer, M. K., Wang, R. H. J., and Weiss, R.: Historical greenhouse gas concentrations for climate modelling (CMIP6), Geoscientific Model Development, 10, 2057–2116, https://doi.org/10.5194/gmd-10-2057-2017, https://www.geosci-model-dev.net/10/2057/2017/, 2017.

Millar, R. J., Otto, A., Forster, P. M., Lowe, J. A., Ingram, W. J., and Allen, M. R.: Model structure in observational constraints on transient climate response, Climatic Change, 131, 199–211, https://doi.org/10.1007/s10584-015-1384-4, http://link.springer.com/10.1007/s10584-015-1384-4, 2015.

Morice, C. P., Kennedy, J. J., Rayner, N. A., Jones, P. D., P., M. C., J., K. J., A., R. N., and D., J. P.: Quantifying uncertainties in global and regional temperature change using an ensemble of observational estimates: The HadCRUT4 data set, Journal of Geophysical Research: Atmospheres, 117, https://doi.org/10.1029/2011JD017187, https://agupubs.onlinelibrary.wiley.com/doi/abs/10.1029/2011JD017187https://www.metoffice.gov.uk/hadobs/hadcrut4/HadCRUT4{_}accepted.pdf, 2011.

Rohde, R., Muller, R. A., Jacobsen, R., Muller, E., Perlmutter, S., Rosenfeld, A., Wurtele, J., Groom, D., and Wickham, C.: A New Estimate of the Average Earth Surface Land Temperature Spanning 1753 to 2011, Geoinformatics & Geostatistics: An Overview, 1, 1, https://doi.org/10.4172/2327-4581.1000101, http://dx.doi.org/10.4172/2327-4581.1000101, 2013.

Sanderson, B.: Relating climate sensitivity indices to projection uncertainty, Earth System Dynamics, 11, 721–735, https://doi.org/10.5194/esd-11-721-2020, https://esd.copernicus.org/articles/11/721/2020/, 2020.

Smith, C.: Effective Radiative Forcing Time Series from the Shared Socioeconomic Pathways, https://doi.org/10.5281/ZENODO.3973015, https://zenodo.org/record/3973015, 2020.

Smith, C. J., Harris, G., Palmer, M. D., Bellouin, N., Myhre, G., Schulz, M., Golaz, J.-C., Ringer, M., Storelvmo, T., and Forster, P. M.: Energy Budget Constraints on the Time History of Aerosol Forcing and Climate Sensitivity, Journal of Geophysical Research: Atmospheres, in submiss, 2020.

Vose, R. S., Arndt, D., Banzon, V. F., Easterling, D. R., Gleason, B., Huang, B., Kearns, E., Lawrimore, J. H., Menne, M. J., Peterson, T. C., Reynolds, R. W., Smith, T. M., Williams, C. N., Wuertz, D. B., Vose, R. S., Arndt, D., Banzon, V. F., Easterling, D. R., Gleason, B., Huang, B., Kearns, E., Lawrimore, J. H., Menne, M. J., Peterson, T. C., Reynolds, R. W., Smith, T. M., Jr., C. N. W., and Wuertz, D. B.: NOAA's Merged Land–Ocean Surface Temperature Analysis, Bulletin of the American Meteorological Society, 93, 1677–1685, https://doi.org/10.1175/BAMS-D-11-00241.1, http://journals.ametsoc.org/doi/abs/10.1175/BAMS-D-11-00241.1, 2012.

Winton, M., Takahashi, K., and Held, I. M.: Importance of Ocean Heat Uptake Efficacy to Transient Climate Change, Journal of Climate, 23, 2333–2344, https://doi.org/10.1175/2009JCLI3139.1, http://journals.ametsoc.org/jcli/article-pdf/23/9/2333/3968777/2009jcli3139{_}1.pdf, 2010.